JACS
JOURNAL OF THE AMERICAN CHEMICAL SOCIETY

COMMUNICATION

pubs.acs.org/JACS

Highly Dispersed Palladium(II) in a Defective Metal−Organic Framework: Application to C−H Activation and Functionalization

Tae-Hong Park,[†] Amanda J. Hickman,[†] Kyoungmoo Koh,[†] Stephen Martin,[†] Antek G. Wong-Foy,[†] Melanie S. Sanford,*[,†] and Adam J. Matzger*[,†,‡]

[†]Department of Chemistry and [‡]Macromolecular Science and Engineering Program, University of Michigan, 930 North University Avenue, Ann Arbor, Michigan 48109, United States

Supporting Information

ABSTRACT: High reversibility during crystallization leads to relatively defect-free crystals through repair of nonperiodic inclusions, including those derived from impurities. Microporous coordination polymers (MCPs) can achieve a high level of crystallinity through a related mechanism whereby coordination defects are repaired, leading to single crystals. In this work, we discovered and exploited the fact that this process is far from perfect for MCPs and that a minority ligand that is coordinatively identical to but distinct in shape from the majority linker can be inserted into the framework, resulting in defects. The reaction of Zn(II) with 1,4-benzenedicarboxylic acid (H_2BDC) in the presence of small amounts of 1,3,5-tris(4-carboxyphenyl)benzene (H_3BTB) leads to a new crystalline material, MOF-5(O_h), that is nearly identical to MOF-5 but has an octahedral morphology and a number of defect sites that are uniquely functionalized with dangling carboxylates. The reaction with $Pd(OAc)_2$ impregnates the metal ions, creating a heterogeneous catalyst with ultrahigh surface area. The Pd(II)-catalyzed phenylation of naphthalene within Pd-impregnated MOF-5(O_h) demonstrates the potential utility of an MCP framework for modulating the reactivity and selectivity of such transformations. Furthermore, this novel synthetic approach can be applied to different MCPs and will provide scaffolds functionalized with catalytically active metal species.

Crystalline microporous coordination polymers (MCPs), and in particular the subset known as metal−organic frameworks (MOFs), have shown extensive potential for use in applications in gas storage,[1] chemical separations,[2] catalysis,[3] sensing,[4] and drug delivery.[5] These MCPs are constructed from the self-assembly of metal ions/clusters and organic linkers under reaction conditions where relatively perfect single-crystal growth is favorable. Despite extensive success with single-linker systems possessing high porosity, coordination copolymerization (as in the use of mixed linkers) has presented tremendous opportunities to control the functionality within the framework[6] and to build new materials with unparalleled surface areas.[7,8] We have reported that two linkers that are coordinatively and topologically identical and have similar reactivities can be randomly copolymerized into the parent MCP structure,[6] whereas two linkers that are coordinatively identical but distinct in shape can form a new, highly porous MCP structure very different from the MCP constructed from either linker.[7] In the latter case, the stoichiometry of the two linkers should be within a certain range of linker mole ratios to obtain a pure phase; if this is not the case, typically the ligand present in highest concentration determines the structure of the resulting MCP. Although the identical coordinating functionality causes the minority linker to be incorporated to some extent, the high reversibility during crystallization repairs such defect sites during synthesis. However, we propose that if the driving force for crystal growth of the majority linker is sufficient, the minority ligand can be inserted into the framework, leading to defects with dangling ligands. In this work, we utilized this approach to produce a new material with a powder X-ray diffraction (PXRD) pattern nearly identical to that of the MCP derived from the dominant linker and displaying comparable gas sorption behavior. This new material possesses a significant number of defect sites that functionalize the pores and show unprecedented reactivity.

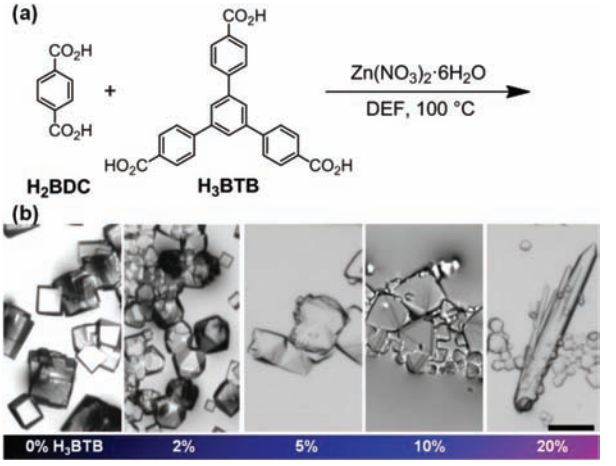

Figure 1. (a) Synthesis of BTB-incorporated MOF-5 crystals by addition of H_3BTB to the reaction mixture of H_2BDC and $Zn(NO_3)_2 \cdot 6H_2O$. (b) Photographs of crystals showing the dependence of the morphology upon the percentage of H_3BTB in the feed (scale bar: 100 μm). Needle-shaped UMCM-1 crystals appear above 10 mol % H_3BTB.

The copolymerization of 1,4-benzenedicarboxylic acid (H_2BDC) and 1,3,5-tris(4-carboxyphenyl)benzene (H_3BTB) (Figure 1) in

Received: October 6, 2011
Published: November 28, 2011

the presence of $Zn(NO_3)_2$ in *N*,*N*-diethylformamide (DEF) provides highly porous, needle-shaped $Zn_4O(BDC)(BTB)_{4/3}$ (UMCM-1) crystals, whereas the same conditions with pure H_2BDC or H_3BTB afford MOF-5 or MOF-177, respectively.[7a] The mole ratio of the two linkers determines the phase obtained. For example, a pure phase of UMCM-1 was obtained at an optimal range of H_2BDC:H_3BTB mole ratios (3:2 to 1:1), whereas a reaction mixture containing ~10 mol % H_3BTB with respect to H_2BDC provided octahedral crystals of MOF-5 as determined by PXRD analysis; the dramatic change in crystal shape was presumed to be an example of an additive-induced morphological change. Here we report, quite surprisingly, that these octahedral MOF-5 crystals differ from MOF-5 in their chemical reactivity rather dramatically and in a manner that is particularly useful for creating heterogeneous catalysts with ultrahigh surface area.

Figure 1 shows the evolution of the crystal morphology with the addition of increasing amounts of H_3BTB to the reaction mixture of H_2BDC and $Zn(NO_3)_2 \cdot 6H_2O$ in DEF. The addition of H_3BTB gradually results in different morphologies from cubic to octahedral. At 2 mol % H_3BTB relative to H_2BDC, truncated cubic or truncated octahedral crystals appear, and at 5−10 mol % H_3BTB, most of the crystals exhibit a uniform octahedral shape. These noncubic crystals show a nearly identical PXRD pattern and the same cubic space group with indistinguishable cell parameters as MOF-5.[7a] Above 10 mol % H_3BTB, needle-shaped UMCM-1 appears concomitantly. The morphology change from cubic to octahedral has been observed in inorganic nanocrystals using a capping reagent.[9] The functional groups on such reagents weakly interact with specific crystal faces, leading to selective changes in the relative rates of growth from different faces.[10] When benzoic acid derivatives having a single carboxylate were added to MOF-5 crystallization, the additives, however, either terminated the crystal growth[11a] or formed holey defects in the cubic crystals.[11b] On the other hand, here a small amount of the tritopic BTB linker appears to regulate the rate and direction of framework extension and crystal growth of MOF-5 without providing the UMCM-1 coordination copolymer.

Despite the PXRD results, NMR measurements revealed the inclusion of BTB in the MOF-5 framework after the crystals were digested in DMSO-d_6 containing DCl [see the Supporting Information (SI)]. The quantity of BTB determined by ^1H NMR analysis was closely correlated with the percentage of H_3BTB in the starting feed. The solvothermal reaction conditions produce diethylamine from thermal degradation of DEF that deprotonates H_2BDC and H_3BTB, leading to the formation of Zn_4O clusters. Whereas the carboxylates in BDC are neutralized in the construction of the MOF-5 framework, only one of the three BTB carboxylates may be incorporated into the Zn_4O cluster as a defect and interrupt the framework extension, leading to octahedral crystals. However, the other two carboxylates of BTB cannot extend the framework. The BET surface areas of 5 and 10% BTB-loaded material were 3070 and 2850 m^2/g, respectively, whereas that of pure MOF-5 synthesized under the same conditions was 3470 m^2/g (see the SI). Although physical entrapment of BTB within MOF-5 as a possible mode of introducing carboxylate functionality cannot be completely ruled out, the replacement of H_3BTB with 1,3,5-tris(4-acetylphenyl)benzene, an isostere for H_3BTB lacking carboxylate functionality, did not lead to incorporation into the structure, as judged by NMR spectroscopy of the acid-digested framework; furthermore, a change in morphology of the crystals was not observed.

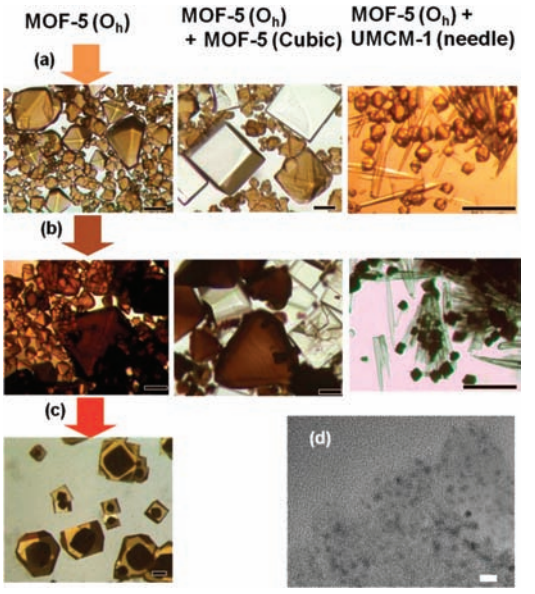

Figure 2. (a) Selective impregnation of Pd(II) ions in MOF-5(O_h) by addition of $Pd(OAc)_2$ in CH_2Cl_2. For comparison, deliberate mixtures of pristine MOF-5 or needle-shaped UMCM-1 with MOF-5(O_h) crystals were tested. (b) Reduction by $NaBH_4$ in DMF. (c) Growth of an IRMOF-3 shell layer on a Pd@MOF-5(O_h) core using H_2ABDC and $Zn(NO_3)_2 \cdot 6H_2O$ in DEF at 85 °C. Scale bars in (a−c): 100 μm. (d) TEM image of Pd@MOF-5(O_h). Scale bar: 5 nm.

Through a mechanism that we ascribe to the presence of uncoordinated carboxylate groups, defective MOF-5 produced with 10% BTB in the feed, designated as MOF-5(O_h), adsorbs a considerable amount of palladium ions from a dilute $Pd(OAc)_2$ solution. A variety of catalytic functions employing different oxidation states and significantly high affinity for H_2 make Pd one of most studied metals to be incorporated into porous solid supports, including MCPs.[12] When MOF-5(O_h) crystals were slowly shaken in a $Pd(OAc)_2$ solution (8.9 mM) in CH_2Cl_2 for 2 days, the colorless crystals became brown and the solution was visibly depleted in Pd. After adsorption in a fresh Pd solution for another 2 days, the crystals were washed with CH_2Cl_2 three times and immersed in CH_2Cl_2 for 2 days, during which time fresh solvent was replenished three times to remove unbound Pd ions. Optical images of Pd-ion-adsorbed MOF-5(O_h), designated as Pd(II)@MOF-5(O_h), are shown in Figure 2. For comparison, MOF-5(O_h) crystals were mixed with pure MOF-5 or UMCM-1 and then placed in a $Pd(OAc)_2$ solution; after 4 days, only MOF-5(O_h) became brown, whereas MOF-5 (cubes) and UMCM-1 (needles) remained nearly colorless. Such selective impregnation suggests that the Pd adsorption is not significant in MOF-5[12f] and UMCM-1 but that the dangling carboxylate groups of MOF-5(O_h) extensively interact with $Pd(OAc)_2$. The NMR spectrum after digestion of Pd(II)@MOF-5(O_h) in acidic DMSO-d_6 revealed the presence of $[Pd(OAc)]^+$ that had exchanged onto the dangling linkers. The Pd content of Pd(II)@MOF-5(O_h) was 2.3 wt %, as determined by inductive coupled plasma optical emission spectroscopy (ICP-OES). Therefore, the above data strongly support the idea that BTB is incorporated into the MOF-5 structure, giving rise to not only a morphology change but also carboxylate functionality within the pores. While the partial degradation of frameworks after Pd incorporation via chemical vapor deposition (CVD)[12a] and infiltration

methods[12b] often significantly reduce surface area, the PXRD and surface area measurements showed that the crystallinity and porosity of MOF-5(O_h) were maintained after the Pd impregnation. The very mild wet chemistry maintained a 2600 m^2/g BET surface area for Pd(II)@MOF-5(O_h). Treatment of Pd(II)@MOF-5(O_h) with $NaBH_4$ in *N*,*N*-dimethylformamide (DMF) reduced Pd^{2+} ions to Pd nanoparticles within the framework, giving a product designated as Pd@MOF-5(O_h). The fairly uniform brown color of cross-sectioned crystals and transmission electron microscopy (TEM) studies suggest that the Pd nanoparticles are evenly distributed throughout the crystals (see the SI and Figure 2d). However, the nearly identical PXRD pattern and surface area (2570 m^2/g) indicate that the framework is still intact after reduction, presenting well-dispersed metal catalysts in a high-surface-area MCP.

Multifunctionality within a single MCP crystal can provide unique applications in catalysts and sensors via regulation of the diffusion rate and size of guest molecules.[13] In this context, core−shell-type crystals were constructed by heating a solution of H_2BDC or 2-amino-1,4-benzenedicarboxylic acid (H_2ABDC) and $Zn(NO_3)_2 \cdot 6H_2O$ to grow a Zn_4OL_3 layer[6a] upon Pd@MOF-5(O_h) seed crystals. The distinct colors of the core and shell indicate the Pd NPs are localized in the core of the crystal (Figure 2c; also see the SI). The replacement of BDC with ABDC presents amine-functionalized pores that can allow further control of pore functionality as well as pore accessibility of the outer layer via postsynthetic modification strategies.[14] Notably, these core−shell crystals exhibit morphology evolution from octahedral to polyhedral, suggesting that a recovery of the native cubic shape is underway.

To illustrate the utility of Pd(II)@MOF-5(O_h) in catalysis, we sought to investigate the material's reactivity for a known Pd(II)-catalyzed reaction. The C−H phenylation of naphthalene using diphenyliodonium tetrafluoroborate was chosen as a test reaction because the reactivity and selectivity have been shown to exhibit a strong dependence on the catalyst structure.[15] Notably, the use of 5 mol % $Pd(OAc)_2$ as the catalyst was shown to result in a low yield and rapid catalyst deactivation. For example, the $Pd(OAc)_2$-catalyzed C−H arylation of naphthalene in nitrobenzene at 120 °C nearly terminated after 30 min, providing a total yield of 13% with 15:1 selectivity for the α isomer over the β isomer. Employing longer reaction times (17 h) improved the yield only slightly and lowered the selectivity (17% yield, α:β = 8:1; Figure 3). We hypothesized that the MCP framework might serve to promote this transformation by slowing the relative rate of catalyst decomposition and/or by stabilizing Pd intermediates during the catalytic cycle.

Indeed, under otherwise identical conditions, the phenylation of naphthalene catalyzed by Pd(II)@MOF-5(O_h) (5 mol % Pd) resulted in a greatly increased yield of phenylated naphthalenes (64%) after 12 h. In contrast to the $Pd(OAc)_2$-catalyzed reaction, the yield of product steadily increased with time, indicating that Pd(II)@MOF-5(O_h) remained catalytically viable significantly longer than $Pd(OAc)_2$. Furthermore, the Pd(II)@MOF-5(O_h)-based catalyst provided significantly different site selectivity (α:β = 3:1) in comparison with $Pd(OAc)_2$. This highlights the exciting promise of the MCP framework for modulating the selectivity of this and other transformations.[16]

Next, potential loss of active Pd species from the crystals was tested. Pd(II)@MOF-5(O_h) crystals were removed from a reaction mixture by hot filtration after heating for 3 h. The isolated solution did not show any further catalytic activity under

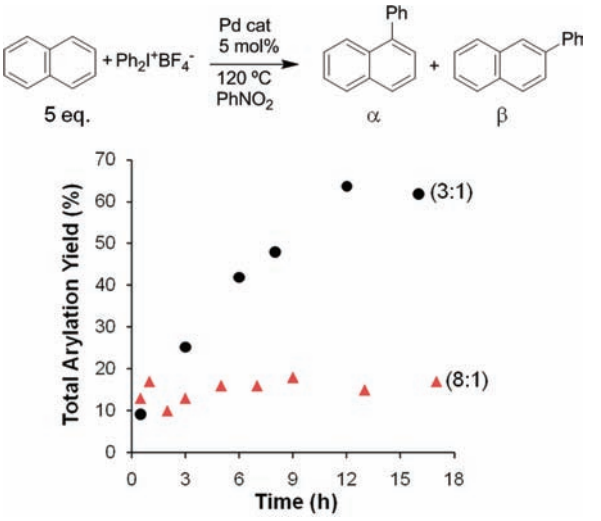

Figure 3. Pd-catalyzed direct phenylation of naphthalene using Pd(II)@MOF-5(O_h) (black ●) or $Pd(OAc)_2$ (red ▲) as the catalyst. The ratio of isomers (α:β) at the end of the reaction is given in parentheses. The Pd loading of Pd(II)@MOF-5(O_h) was 2.3 wt % as determined by ICP-OES, and the yield and selectivity were determined by GC−MS using an internal standard.

the same reaction conditions. In addition, nitrobenzene containing only Pd(II)@MOF-5(O_h) was heated for 3−16 h, and the solid was removed by hot filtration. Naphthalene and oxidant were added to the filtrate, and the mixture was heated for 12 h, giving only 2−8% of phenylated products. These results suggest that diffusion of the Pd catalyst out of the solid support is negligible.

PXRD studies of solid recovered from the reactions (see the SI) showed that the MOF-5(O_h) framework gradually degraded with reaction time, although Pd(II)@MOF-5(O_h) did not lose crystallinity under the same conditions when either of the reactants was not present in the solution. After 12 h, the crystallinity of the MCP completely disappeared, and the arylation also terminated. A TEM study of solid collected from the reaction showed that ∼20 nm Pd nanoparticles were spread over noncrystalline solid, leading to broad Pd metal reflections in the PXRD pattern at 40.2 and 46.5°. Such MCP decomposition suggests that defect inclusion in more robust MCP crystals will be useful in producing improved catalysts for direct C−H arylation. Additionally, only modest site selectivity was observed for the Pd(II)@MOF-5(O_h)-catalyzed naphthalene arylation, and exploration of the influence of pore size and shape is an attractive future direction. Previous investigations of diimine Pd(II) catalysts for this transformation suggest that further optimization of the coordination environment of the palladium active site via modification of the MCP crystal could also dramatically increase the selectivity.[15]

In conclusion, defects in MOF-5 can be produced by the addition of a small amount of H_3BTB during synthesis; this leads to a new material nearly identical to MOF-5 but having an octahedral morphology. The resulting framework is uniquely functionalized with carboxylates of the dangling linkers and extensively differs from MOF-5 in reactivity toward Pd ions, leading to heterogeneous catalysts with ultrahigh surface area. This novel synthetic approach can be further applied to different MCPs providing scaffolds for impregnation of catalytically active metal species.

■ ASSOCIATED CONTENT

Supporting Information. Synthesis, characterization, and N_2 isotherm measurements of MCPs; procedure for Pd(II)@MOF-5(O_h)-catalyzed phenylation of naphthalene; and complete ref 5b. This material is available free of charge via the Internet at http://pubs.acs.org.

■ AUTHOR INFORMATION

Corresponding Author
mssanfor@umich.edu; matzger@umich.edu

■ ACKNOWLEDGMENT

This material is based upon work supported by the U.S. Department of Energy (DE-SC0004888 to A.J.M. and A.G.W.-F. and DE-FG02-08ER 15997 to M.S.S.). In addition, A.J.H. thanks the National Science Foundation for a graduate fellowship.

■ REFERENCES

(1) (a) Millward, A. R.; Yaghi, O. M. *J. Am. Chem. Soc.* **2005**, *127*, 17998–17999. (b) Wong-Foy, A. G.; Matzger, A. J.; Yaghi, O. M. *J. Am. Chem. Soc.* **2006**, *128*, 3494–3495. (c) Caskey, S. R.; Wong-Foy, A. G.; Matzger, A. J. *J. Am. Chem. Soc.* **2008**, *130*, 10870–10871.

(2) (a) Cychosz, K. A.; Ahmad, R.; Matzger, A. J. *Chem. Sci.* **2010**, *1*, 293–302. (b) Ahmad, R.; Wong-Foy, A. G.; Matzger, A. J. *Langmuir* **2009**, *25*, 11977–11979.

(3) (a) Lee, J.; Farha, O. K.; Roberts, J.; Scheidt, K. A.; Nguyen, S. T.; Hupp, J. T. *Chem. Soc. Rev.* **2009**, *38*, 1450–1459. (b) Ma, L.; Abney, C.; Lin, W. *Chem. Soc. Rev.* **2009**, *38*, 1248–1256.

(4) Xie, Z.; Ma, L.; deKrafft, K. E.; Jin, A.; Lin, W. *J. Am. Chem. Soc.* **2010**, *132*, 922–923.

(5) (a) An, J.; Geib, S. J.; Rosi, N. L. *J. Am. Chem. Soc.* **2009**, *131*, 8376–8377. (b) Horcajada, P.; et al. *Nat. Mater.* **2010**, *9*, 172–178.

(6) (a) Koh, K.; Wong-Foy, A. G.; Matzger, A. J. *Chem. Commun.* **2009**, 6162–6164. (b) Park, T.-H.; Koh, K.; Wong-Foy, A. G.; Matzger, A. J. *Cryst. Growth Des.* **2011**, *11*, 2059–2063.

(7) (a) Koh, K.; Wong-Foy, A. G.; Matzger, A. J. *Angew. Chem., Int. Ed.* **2008**, *47*, 677–680. (b) Koh, K.; Wong-Foy, A. G.; Matzger, A. J. *J. Am. Chem. Soc.* **2009**, *131*, 4184–4185. (c) Koh, K.; Wong-Foy, A. G.; Matzger, A. J. *J. Am. Chem. Soc.* **2010**, *132*, 15005–15010.

(8) Furukawa, H.; Ko, N.; Go, Y. B.; Aratani, N.; Choi, S. B.; Choi, E.; Yazaydin, A. O.; Snurr, R. Q.; O'Keeffe, M.; Kim, J.; Yaghi, O. M. *Science* **2010**, *329*, 424–428.

(9) Tao, A.; Sinsermsuksakul, P.; Yang, P. D. *Angew. Chem., Int. Ed.* **2006**, *45*, 4597–4601.

(10) Surfactant-assisted controlled crystallization of MOF-5 recently provided nanosized octahedral MOF-5. See: Ma, M.; Zacher, D.; Zhang, X.; Fischer, R. A.; Metzler-Nolte, N. *Cryst. Growth Des.* **2011**, *11*, 185–189.

(11) (a) Hermes, S.; Witte, T.; Hikov, T.; Zacher, D.; Bahnmuller, S.; Langstein, G.; Huber, K.; Fischer, R. A. *J. Am. Chem. Soc.* **2007**, *129*, 5324–5325. (b) Choi, K. M.; Jeon, H. J.; Kang, J. K.; Yaghi, O. M. *J. Am. Chem. Soc.* **2011**, *133*, 11920–11923.

(12) (a) Hermes, S.; Schroter, M. K.; Schmid, R.; Khodeir, L.; Muhler, M.; Tissler, A.; Fischer, R. W.; Fischer, R. A. *Angew. Chem., Int. Ed.* **2005**, *44*, 6237–6241. (b) Sabo, M.; Henschel, A.; Froede, H.; Klemm, E.; Kaskel, S. *J. Mater. Chem.* **2007**, *17*, 3827–3832. (c) Hwang, Y. K.; Hong, D. Y.; Chang, J. S.; Jhung, S. H.; Seo, Y. K.; Kim, J.; Vimont, A.; Daturi, M.; Serre, C.; Férey, G. *Angew. Chem., Int. Ed.* **2008**, *47*, 4144–4148. (d) Cheon, Y. E.; Suh, M. P. *Angew. Chem., Int. Ed.* **2009**, *48*, 2899–2903. (e) Zlotea, C.; Campesi, R.; Cuevas, F.; Leroy, E.; Dibandjo, P.; Volkringer, C.; Loiseau, T.; Férey, G.; Latroche, M. *J. Am. Chem. Soc.* **2010**, *132*, 2991–2997. (f) Kleist, W.; Maciejewski, M.; Baiker, A. *Thermochim. Acta* **2010**, *499*, 71–78. (g) Bloch, E. D.; Britt, D.; Lee, C.; Doonan, C. J.; Uribe-Romo, F. J.; Furukawa, H.; Long, J. R.; Yaghi, O. M. *J. Am. Chem. Soc.* **2010**, *132*, 14382–14384. (h) Hermannsdörfer, J.; Kempe, R. *Chem.—Eur. J.* **2011**, *17*, 8071–8077. (i) Li, H.; Zhu, Z.; Zhang, F.; Xie, S.; Li, H.; Li, P.; Zhou, X. *ACS Catal.* **2011**, *1*, 1604–1612.

(13) Zacher, D.; Schmid, R.; Woll, C.; Fischer, R. A. *Angew. Chem., Int. Ed.* **2011**, *50*, 176–199.

(14) Wang, Z.; Cohen, S. M. *Chem. Soc. Rev.* **2009**, *38*, 1315–1329.

(15) Hickman, A. J.; Sanford, M. S. *ACS Catal.* **2011**, *1*, 170–174.

(16) (a) Only a small background reaction was observed in the presence of unmetalated MOF-5(O_h) (resulting in 7% yield, 5:1 selectivity after 16 h). (b) The presence of MOF-5 crystals in a homogeneous catalyst reaction with $Pd(OAc)_2$ only slightly improved the yield (21%) with a parallel selectivity (8:1) after 16 h (see the SI).